Creeping yeast: a simple, cheap, and robust protocol for the identification of mating type in *Saccharomyces cerevisiae*

Samantha D. M. Arras[1], Taylor R. Hibbard[2], Lucy Mitsugi-McHattie[1], Matthew A. Woods[3], Charlotte E. Johnson[1], Andrew Munkacsi[2], Sylvie Hermann-Le Denmat[1*], and Austen R. D. Ganley[1,3,4*]

[1]School of Biological Sciences, University of Auckland, Auckland, 1142, New Zealand

[2]School of Biological Sciences, Victoria University of Wellington, Wellington 6012, New Zealand

[3]Digital Life Institute, University of Auckland 0632, New Zealand

[4]Institute of Natural and Mathematical Sciences, Massey University, Auckland 0632, New Zealand

*Correspondence email: a.ganley@auckland.ac.nz ; s.hermann@auckland.ac.nz

Abstract

Saccharomyces cerevisiae is an exceptional genetic system, with genetic crosses facilitated by its ability to be maintained in haploid and diploid forms. Such crosses are straightforward if the mating type/ploidy of the strains are known. Several techniques can be used to determine mating type (or ploidy), but all have limitations. Here we validate a simple, cheap and robust method to rapidly identify *S. cerevisiae* mating types. When cells of opposite mating type are mixed in liquid media, they "creep" up the culture vessel sides, a phenotype that can be easily detected visually. In contrast, mixtures of the same mating type or with a diploid simply settle out. The phenotype is robust to different media, cell densities, temperatures and strains, and is observable for several days. Microscopy suggests that cell aggregation during mating is responsible for the phenotype. Yeast knockout collection analysis identified 107 genes required for the creeping phenotype, with these being enriched for mating-specific genes. Surprisingly, the RIM101 signalling pathway was strongly represented. We propose that RIM101 signalling regulates aggregation as part of a wider, previously-unrecognized role in mating. The simplicity and robustness of this method makes it ideal for routine verification of *S. cerevisiae* mating type, with future studies required to verify its molecular basis.

Introduction

The ability to maintain *Saccharomyces cerevisiae* in haploid and diploid forms as well as to perform genetic crosses is fundamental to the success of this yeast as a model organism for molecular genetics (Guthrie & Fink, 1991, Botstein & Fink, 2011). *S. cerevisiae* has two mating types, **a** and α. In nature *S. cerevisiae* is predominately inbreeding, as it routinely switches mating-type to overcome mating-type incompatibility (Haber, 2012). However, in most laboratory *S. cerevisiae* strains mating type is extremely stable and heritable due to deletion of the *HO* endonuclease gene that facilitates this mating type switching (Herskowitz & Jensen, 1991). Mating type is determined by which of two idiomorphs (termed as such because of differences in length and sequence), *MAT***a** or *MAT*α, is present at the *MAT* locus (Haber, 2012). The *MAT*α idiomorph encodes two genes that specify the α-specific phenotype, while the *MAT***a** idiomorph encodes a transcriptional repressor that, in **a**/α diploids, suppresses expression of haploid-specific genes. Haploid cells respond to the mating type pheromones produced by the opposite mating type, triggering a signalling cascade that eventually results in morphological changes that drive cell fusion and karyogamy (Bardwell, 2005).

Mating between compatible *S. cerevisiae* cells in liquid cultures involves an aggregation process that physically holds cells together. This sexual aggregation is mediated by **a** and α agglutinin proteins that are expressed on the surface of the cell wall of haploid **a** and α strains, respectively (Banderas *et al.*, 2016). The **a**-agglutinin is composed of two subunits encoded by the *AGA1* and *AGA2* genes, while the α-agglutinin is encoded by *SAG1* (Lipke & Kurjan, 1992). The agglutinin proteins adhere once they come into contact with each other like a sort of molecular Velcro that promotes cell-cell contact (Lipke & Kurjan, 1992). Agglutinins are constitutively expressed at low levels, with their expression being up-regulated in response to

41 mating-type pheromone to facilitate cell aggregation (Lipke & Kurjan, 1992). The sexual
42 aggregation mediated by these agglutinins is likely the first step for mating of yeast cells mixed
43 in suspension (Banderas *et al.*, 2016).

44

45 Performing genetic crosses in *S. cerevisiae* relies on knowing the mating types of the haploid
46 strains involved. While the mating type and ploidy of established laboratory strains are
47 generally known, there are a number of scenarios where they need to be determined. This
48 includes when dissecting ascospores to produce haploid strains, checking the mating of strains
49 that lack convenient markers, or when mutating the *HO* locus in wild-type strains. Currently,
50 several methodologies are used to determine mating type and ploidy. Flow cytometry can be
51 used to determine if a cell is haploid or diploid, but does not distinguish mating type. A simple
52 method to determine mating type or ploidy is to spread cells following mating on selective
53 medium to look for cells containing markers from both parents, although this obviously
54 requires appropriate markers (Sherman, 1991). A PCR method utilizes *MAT* locus primers that
55 produce different amplicon sizes depending on which mating type idiomorph is present
56 (Bradbury *et al.*, 2006). Microscopic observation of the 'shmoo' phenotype, which is a
57 manifestation of morphological changes induced upon detection of the opposite mating type
58 pheromone, is also used to identify mating type (Duntze *et al.*, 1970, Sprague, 1991, Merlini
59 *et al.*, 2013) following mixing of known *MAT***a** or *MAT*α strains with the unknown strain(s).
60 However, shmoo formation can be transient and is only observed in a small number of cells.
61 Finally, the "halo" method, which relies on inhibition of certain strains by pheromone
62 production, can be used to determine mating type but requires tester strains with specific
63 genotypes (Sprague, 1991). Thus, although there is a diversity of methods, they are time-
64 consuming, require specific components, and/or can produce inconsistent or transient results.

Here, we demonstrate a simple, cheap and robust method to enable the rapid identification of the mating type and ploidy of *S. cerevisiae* strains. The principle of the method is that when cells of opposite mating type are mixed, they "creep" up the sides of the culture vessel in an easily observable manner, unlike mixtures involving the same mating type or a diploid strain, which simply settle out. An unknown strain can be mixed with known strains of each mating type in a culture medium, left overnight, and simply observed to allow accurate distinction of both mating types as well as of diploid strains. The response is long-lasting, does not require specialized equipment or reagents, and requires minimal hands-on time. Investigation of the molecular basis for this 'creeping' phenotype using microscopy and the yeast knockout collection suggests that it is a consequence of cell aggregation, and indicates a surprising role of the RIM101 pathway in *S. cerevisiae* mating.

77 **Methods**

78 **Yeast strains and standard growth conditions**

79 All strains used in this study are listed in **Supplementary Table 1**. Culture media used were
80 YPD (1% yeast extract, 2% bacto-peptone and 2% glucose), YPGlycerol (1% yeast extract, 2%
81 bacto-peptone and 2% glycerol), and YNB (0.45% yeast nitrogen base with ammonium
82 sulphate, appropriate amino acids and bases, and 2% glucose (Treco & Lundblad, 1993);
83 **Supplementary Table 2**). Strains were stored in 15% glycerol at -80˚C until use.

84

85 **Mating type assay**

86 Strains were revived from glycerol stocks on YPD medium then grown overnight in appropriate
87 liquid medium (YPD unless stated otherwise) at 30˚C. Strains were diluted to OD_{600nm} 0.2 in
88 the same medium and added in equal volumes to a tube (2 mL per strain for a test tube, 250 µL
89 for a microcentrifuge tube, or 100 µL for a 96-well plate). Cultures were left with no shaking
90 for approximately 18 hrs at ~22˚C (room temperature) unless otherwise indicated, after which
91 they were observed and photographed. Time-lapse photography was performed using a Nikon
92 D850 camera with a 60 mm macro lens and polarizing filter. Images were exposed at ISO200,
93 f/16 for 10 s. Photographs were taken every minute from the start of the experiment for 20 hrs.
94 Microscopic observation of cell aggregation was carried out for mating and non-mating cells
95 using a LEICA ICC50 W microscope and the Leica Application Suite (LAS) EZ software
96 (Leica Microsystems v3.2). Observations were performed on 10 µL of 200 µL mating and non-
97 mating cell mixtures from a 96-well plate incubated on the bench with no shaking. Each 10 µL
98 sample was gently collected from the bottom of the well where the creeping phenotype is seen
99 and observed hourly from 2 to 7 hrs following mixing.

100

101 **Multiplex PCR to confirm mating type assay**

102 Primers MAT-a 5'-CAATGATTAAAATAGCATAGTCGG-3', MAT-alpha 5'-
103 CAGCACGGAATATGGGAC-3' and MAT-R 5'-GGTGCATTTGTCATCCGTC-3'
104 (Bradbury *et al.*, 2006) were used in a multiplex PCR reaction to amplify mating-type specific
105 PCR products from 2 µL of overnight yeast culture (100 µL in YPD) in a final volume of 25
106 µL. PCR was performed with the KAPA2G Robust DNA polymerase in GC buffer (Custom
107 Science). Cycling parameters were initial incubation of 10 mins at 94˚C, then 35 cycles of 94˚C
108 for 25 s, 55˚C for 25 s and 72˚C for 90 s. The *MAT***a** amplicon (489 bp) and *MAT*α amplicon
109 (466 bp) were visualized on a 3% agarose gel run at 100 V for 4 hrs in sodium borate buffer
110 (10 mM NaOH, 36 mM boric acid) and stained with ethidium bromide.

111

112 **Genome-wide analysis of the mating type assay**

113 The genetic basis for the "creeping" phenotype was investigated via crosses of BY4742
114 (*MAT*α) with the gene deletion library (*MAT***a**; BY4741 as parental strain) in round bottom 96-
115 well plates. First, the gene deletion library (Open Biosystems) was incubated overnight at 30˚C
116 in 200 µL YPD, and BY4742 was incubated overnight at 30˚C in 5 mL YPD. The next day, 80
117 µL of BY4742 cells (1.26 x 10^7 cells/mL) was mixed with 120 µL of gene deletion library
118 strains, incubated overnight at 30˚C, and imaged using a digital camera. Mating and non-
119 mating phenotypes were identified through independent visual inspection by two people.

120

121 **Phenotype enrichment**

Genes required for the "creeping" phenotype were analyzed for phenotype enrichment using YeastEnrichr (Chen *et al.*, 2013, Kuleshov *et al.*, 2016). Functional enrichment for phenotype was evaluated using text-mining associations of each gene with phenotypes reported in publications in PubMed. Significant enrichment was defined for categories with an adjusted *P*-value, a z-score (expected:observed ratio for each phenotype), and a combined score (the product of the z-score and negative logarithm of the *P*-value).

Spatial analysis of functional enrichment

Genes required for the "creeping" phenotype were annotated for placement in a functionally annotated genetic interaction network (Costanzo *et al.*, 2016) via spatial analysis of functional enrichment (SAFE; Baryshnikova, 2016).

Network analysis

Genes required for the "creeping" phenotype were annotated for function via network- and pathway-based community partitioning as previously described (Busby *et al.*, 2019). Using NetworkAnalyst (Zhou *et al.*, 2019), genes were mapped in a first-order network within an established yeast global interaction network (the STRING interactome; Szklarczyk *et al.*, 2015) with a confidence cutoff of 900 and requirement for experimental evidence. Significant community modules ($P < 0.05$) were identified using the InfoMap algorithm, and pathways enriched in these modules were determined using KEGG pathway (Kanehisa & Goto, 2000, Kanehisa *et al.*, 2021) analysis (FDR < 0.05).

144 **Results and Discussion**

145 **A quick and reliable assay for determination of mating type in *S. cerevisiae***

146 Routine observations in our laboratory showed that *S. cerevisiae* cells of different mating types
147 settled in non-shaking cultures differently to cells of the same mating type. The manifestation
148 of this mating type phenotype is that cultures of *S. cerevisiae* cells of opposite mating types
149 consistently "creep" up the sides of the culture vessel when mixed and left overnight on the
150 bench with no shaking (**Figure 1**). This "creeping" phenotype is not observed in cultures with
151 a mixture of cells of the same mating type (**a** or α), or where one or both cultures are diploid -
152 these instead simply settle to the bottom of the vessel (**Figure 1**).

153

154 We decided to investigate this observation further using a variety of vessels to determine
155 whether it could form a robust mating type assay. We found that the creeping phenotype is
156 observed in glass test tubes, plastic microfuge tubes, and round bottom microwell plates
157 (**Figure 1A-C**), demonstrating its scalability and flexibility, although we did not observe the
158 phenotype in flat-bottomed microwell plates. Time-lapse photography revealed that the
159 formation of the creeping phenotype is visible ~4 hrs after the mixing of YPD cultures of **a** and
160 α cells at room temperature, and intensifies between about 4 and 8 hrs (**Figure 1D**; see
161 **Supplementary Movie** for a complete video of the formation of the creeping phenotype over
162 20 hrs). Moreover, the phenotype is visible for several days. These results show that this assay
163 is a simple way to distinguish *MAT***a** and *MAT*α strains (formation of the creeping phenotype
164 with one or other of the known mating type tester strains), as well as diploid strains (no creeping
165 phenotype with either known mating type tester strain), and that the assay can be performed in
166 a variety of culture vessel formats.

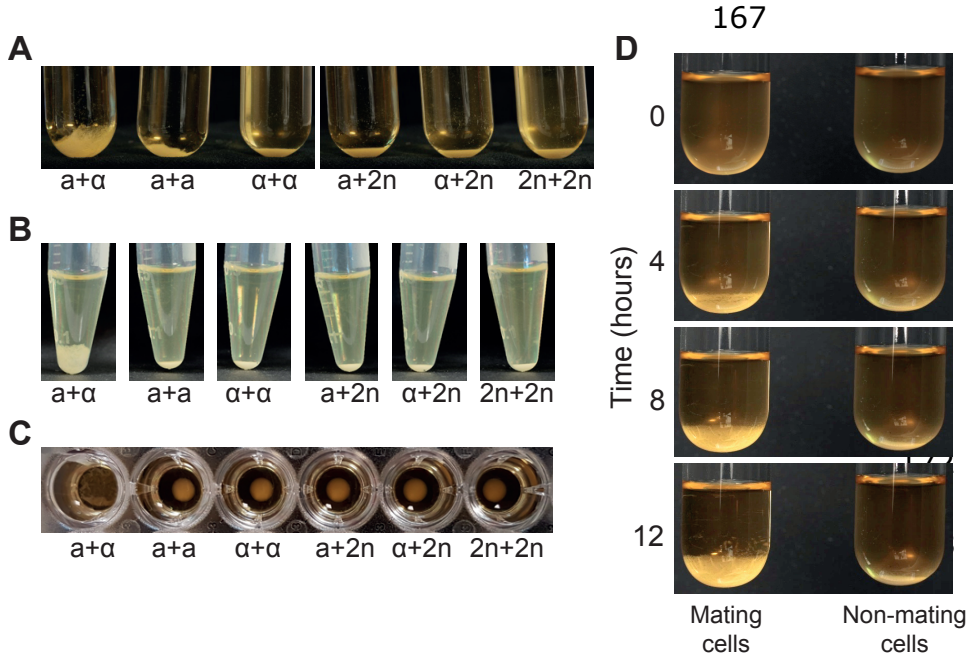

Figure 1: A 50:50 mixture of a+α cells reveals a creeping phonotype. YPD cultures (OD_{600nm} 0.2) were mixed in equal volumes of: 2 mL each in 20 mL glass tubes (**A**); 250 µL each in microcentrifuge tubes (**B**); and 100 µL each in a round-bottomed 96-well plate (**C**). Mixtures were allowed to settle on the bench for 18 hrs and photographed. The creeping phenotype is only observed for the mixtures of opposite mating types (**a**+α). Mating types **a** (a) and α (α), and diploid cells (2n) are indicated below the tubes. The phenotype was not observed in flat-bottomed 96-well plates. **(D)**. Time-lapse photographs of an **a**+α assay at 0, 4, 8, and 12 hrs show the formation of the creeping phenotype compared to a tight pellet for non-mating cells. For full time lapse over 20 hrs, see **Supplementary Figure 1**, and for a video, see **Supplementary Movie**.

Determination of conditions compatible with the mating type assay

We next wanted to characterize how robust the mating type phenotype is under different conditions to assess its practicality as a mating type assay. We first tried different media, including rich and synthetic media, and water. The creeping phenotype forms reliably in both rich and synthetic media containing glucose as the carbon source, but is less obvious when glycerol is used and does not manifest in water (**Figure 2A**). Next we tested the effects of cell density and partner ratio on the phenotype for cells grown in glucose rich medium. Cell density

can be varied from 0.2 to 1.8 (OD_{600nm}) without affecting the formation of the creeping phenotype (**Figure 2B**), while increasing the proportion of one partner over 60% impedes the creeping phenotype (**Figure 2C**). The assay is symmetric, in that disruption of the creeping phenotype is observed equally regardless of which partner (**a** or α) is present in excess (**Supplementary Figure 2**). Interestingly, detection of the creeping phenotype is improved in 96-well plates compared to tubes (compare **Supplementary Figure 2** to **Figure 2C).** Finally, the creeping phenotype is obvious at temperatures in the optimal growth range for *S. cerevisiae* (~22˚C and 30˚C), but is nevertheless still visible when the cultures are incubated at 37°C (**Figure 2D**). However, as for cells in water, formation of the creeping phenotype does not occur at 4˚C (**Figure 2D**).

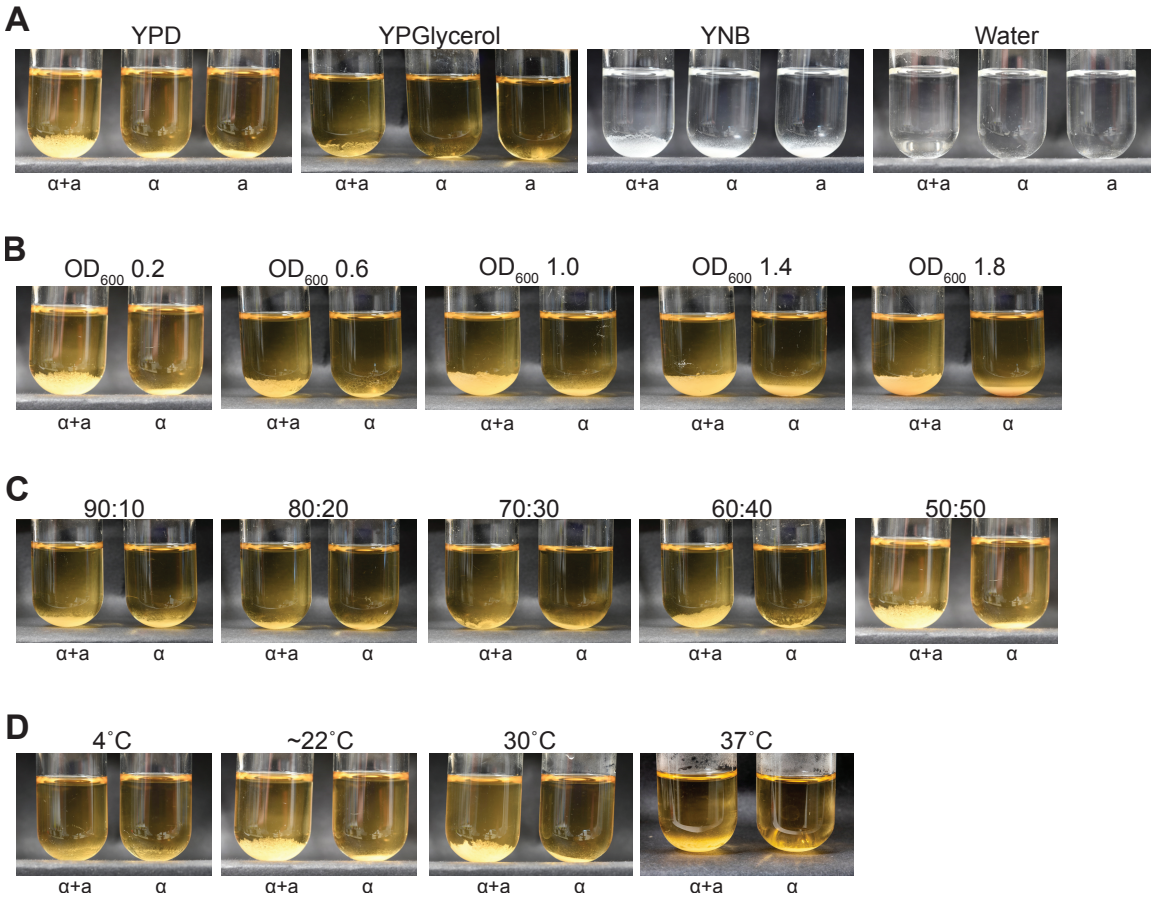

204 **Figure 2: Establishing working parameters for the mating assay.** Four parameters were varied: medium (**A**),
205 cell density (**B**), partner ratio (**C**), and temperature (**D**). Strains were diluted to OD_{600} 0.2 in YPD, mixed equally
206 (50:50) and incubated at room temperature (~22˚C) unless otherwise indicated. Mating type **a** (a) and mating type
207 α (α) cells are indicated below the tubes. All mixtures were photographed at 18 hrs. (**A**) Overnight YPD cultures
208 were diluted in the indicated media or water prior to the mating assay. Note that YNB and water appear this color
209 because of medium composition, not black and white photography. (**B**) The same overnight YPD cultures from
210 (**A**) were diluted to OD_{600nm} 0.2, 0.6, 1.0, 1.4, or 1.8 to perform the assay. **(C)** Opposite mating type cells were
211 mixed at the different ratios indicated in a final volume of 4 mL (ratios represent α:**a**; see **Supplementary Figure**
212 **2** for the reciprocal ratios). (**D***)* Mixtures were incubated at 4˚C, room temperature, 30˚C or 37˚C for 18 hrs. Note
213 that the first panel in (**A**) and in (**B**), the last panel in (**C**), and the second panel in (**D**) are all the same.

214

215 **Mating type determination of different strains of *S. cerevisiae***

216 To assess how robust the assay is to strain type, fourteen *S. cerevisiae* strains derived from
217 different wild isolates (Cubillos *et al.*, 2009) that include representatives of each of the five
218 major, non-mosaic *S. cerevisiae* clades described by Liti *et al.* (2009) were selected
219 (**Supplementary Table 1**). To test whether the assay is able to determine their mating types,
220 each strain was individually mixed with known tester **a** and α strains using standard conditions
221 (YPD medium, OD_{600nm} 0.2, overnight incubation on the bench without shaking). The length
222 of incubation time necessary to unambiguously visualize the creeping phenotype varied
223 depending on the growth rate of the strain. The mating type determinations made using this
224 assay matched that recorded for each strain, with one exception (**Figure 3A; Supplementary**
225 **Figure 3**). The one exception is illuminating: we found a discrepancy between the mating type
226 determined by us and that expected (strain 1; *MAT*α by our assay but expected to be *MAT***a**;
227 **Supplementary Table 1**). To check this strain and validate the mating type determinations,
228 we carried out multiplex PCR on seven strains with primers previously designed to determine
229 the presence of the **a** or α idiomorph within the active *MAT* locus (Bradbury *et al.*, 2006). Each

strain gave the 489 bp **a** or 466 bp α band expected from the creeping phenotype assay (**Figure 3B**), including the discrepant strain. Therefore, this discrepant strain is *MAT*α as the creeping phenotype suggests, with the discrepancy likely a strain designation error rather than a problem with the assay. Together, these results show that the assay can accurately determine mating type for a variety of *S. cerevisiae* strains under a variety of conditions.

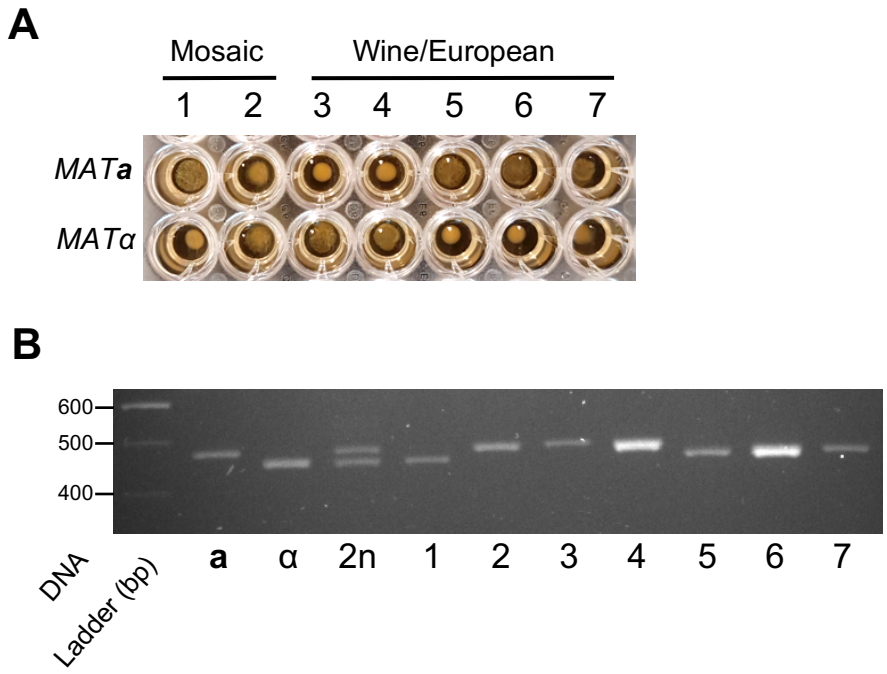

Figure 3: Determination of mating type of wild *S. cerevisiae* strains. (A) Seven strains from the Mosaic and Wine/European clades identified in Liti *et al.* (2009) were mixed with *MAT***a** and *MAT*α tester strains using standard assay conditions (YPD medium, OD_{600nm} 0.2, room temperature incubation). Mixtures were photographed after 18 hrs. The creeping phenotype is visible for strains 1, 5, 6 and 7 crossed with *MAT***a** tester but not with *MAT*α tester. The opposite result is visible for strains 2, 3 and 4. (**B**) Mating assay results were confirmed by multiplex PCR carried out on cells from the seven strains and tester **a**, α and 2n strains. Expected *MAT***a** and *MAT*α specific amplicons are 489 bp and 466 bp, respectively. As expected, both amplicons are observed in the diploid strain. Seven additional strains are shown in **Supplementary Figure 3**.

Sexual aggregation is implicated in the creeping phenotype

To shed light on the basis of the creeping phenotype, we made microscopic observations of the cells as the cultures began to creep. These observations show increased aggregation of cells with time when both mating types are present, but not when only one mating type is present (**Figure 4; Supplementary Figure 4**). Therefore, these results implicate aggregation as the basis for the creeping phenotype. This is consistent with the nature of the phenotype (cells "moving" up the vessel sides through adherence and growth), the requirement for a medium supporting growth, the poor performance on glycerol (which is not a favored carbon source for *S. cerevisiae*), the absence of the phenotype at 4˚C (sexual aggregation has previously been reported to be cold sensitive (Zhao *et al.*, 2001)), and the phenotype becoming evident from ~4 hrs (around the time of mating initiation (Duntze *et al.*, 1970, Sena *et al.*, 1973)).

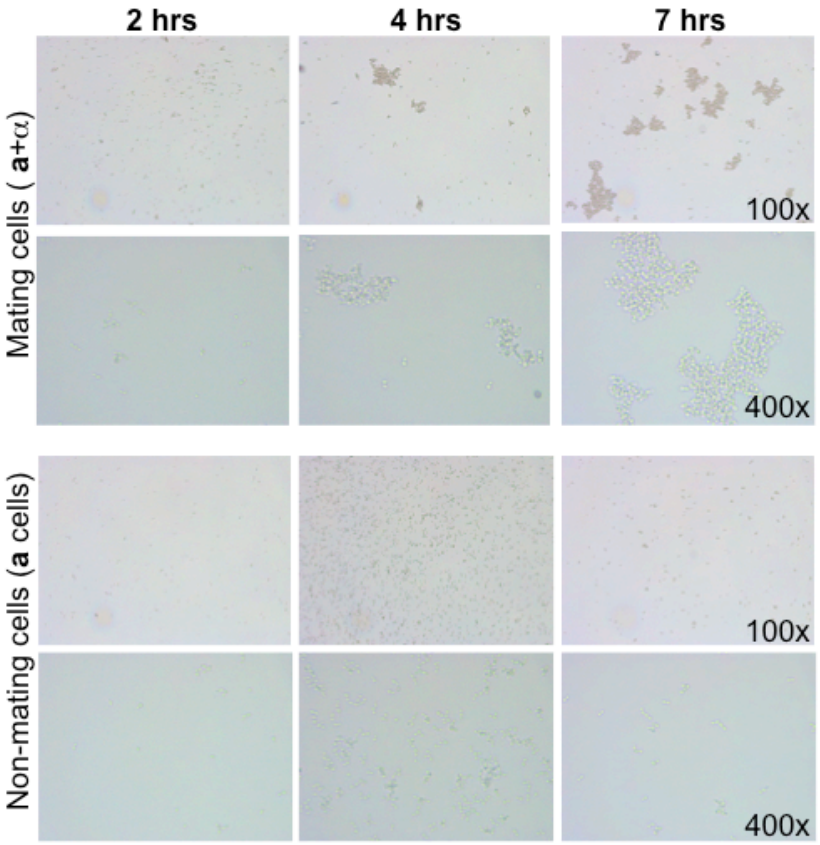

Figure 4: Creeping cells aggregate over time. Mating and non-mating samples of **a**+α cells or haploid **a** cells

267 were observed under the microscope. Images were taken from 2 to 7 hrs after cells were mixed. Representative
268 images at 100x and 400x magnification are shown. Extensive cell aggregation is observed for mating cells from
269 4 hrs following mixing, while no appreciable aggregation is observed for non-mating cells over the same time
270 period. See **Supplementary Figure 4** for the full time course.

271

272 **Functional genomics confirms the creeping phenotype is associated with mating**

273 To gain further insight into the mechanism behind the creeping phenotype, we used a yeast
274 deletion library (Giaever & Nislow, 2014) to examine the impact of non-essential gene
275 deletions on the ability to produce the creeping phenotype. To do this, we mated 4,294 haploid
276 gene deletion strains in a *MAT***a** background void of any growth defect with a wild-type *MAT*α
277 strain, performing two biological replicate experiments. From this we identified 107 gene
278 deletion strains that failed to produce the creeping phenotype in either replicate
279 (**Supplementary Table 3**). These 107 genes comprised 84 characterized genes, and 23
280 uncharacterized open reading frames (ORFs) that encode putative proteins, dubious ORFs, or
281 proteins of unknown function.

282 As expected, the 107 genes required for the creeping phenotype are strongly enriched for genes
283 involved in yeast mating. This conclusion is supported by the results of an unbiased assessment
284 of the genetics underlying the creeping phenotype. This was performed by using YeastEnrichr
285 (Kuleshov *et al.*, 2016) to identify over-represented phenotypes associated with the 107 genes
286 compared to random gene sets. The top four functions (by adjusted P-value < 0.05) are all
287 involved in mating (mating efficiency, mating response, pheromone production and pheromone
288 sensitivity), as are other highly enriched functions such as nuclear fusion during mating and
289 shmoo formation (**Supplementary Table 4**). Moreover, most of the genes reported to be
290 involved in mating signalling (Merlini *et al.*, 2013) were amongst our 107 gene set, although
291 none of the genes involved in cell-cell fusion were (**Table 1**). This enrichment in mating

292 signalling but not cell fusion is consistent with the creeping phenotype resulting from
293 aggregation, which occurs before fusion. Surprisingly given the deletion collection is *MAT***a**,
294 *STE2* that encodes the receptor for pheromone α (Burkholder & Hartwell, 1985) was not
295 amongst our 107 genes (**Table 1**). However, it has been reported that strains deleted for *STE2*
296 display a low background of mating (Jahng *et al.*, 1988), which might explain the persistence
297 of the creeping phenotype in absence of *STE2*. Conversely, the inclusion of *MFA1* amongst our
298 107 genes (**Table 1**) is surprising considering that *MFA1* and *MFA2* both encode the **a**
299 pheromone and were shown to be functionally redundant (Michaelis & Herskowitz, 1988). This
300 might suggest that *MFA2* is not able to compensate for the absence of *MFA1* whereas *MFA1*
301 can compensate for the absence of *MFA2* to produce the creeping phenotype, which is
302 consistent with *MFA2* producing three-fold less **a** pheromone than *MFA1* (Chen *et al.*, 1997).
303 Finally, consistent with the evidence implicating aggregation, we found that the creeping
304 phenotype was not detectable in the absence of the *AGA1* or *AGA2* agglutinin genes
305 (**Supplementary Table 3**). Thus, as expected, the creeping phenotype seems to depend on
306 yeast mating genetic pathways and the genetic results are consistent with the involvement of
307 mating aggregation.

308

309

310 **Table 1**. Overlap between mating signalling/cell-cell fusion genes and genes required for the
311 creeping phenotype

Function	Gene	Note
SIGNALLING COMPONENTS		
Pheromone **a**	*MFA1*[a], *MFA2**	
Pheromone α	*MF(ALPHA)1*[b] *MF(ALPHA)2*	α specific gene[c] α specific gene
G-protein coupled receptors		
Receptor for pheromone **a**	*STE3*	α specific gene
Receptor for pheromone α	*STE2**	
G-protein α subunit	*GPA1*	
G-protein β subunit	*STE4*	
G-protein γ subunit	*STE18*[d]	Not in the YKO library
PAK kinase	*STE20*	
MAPK scaffold	*STE5*	
MAPK scaffold	*STE50*	
MAPKKK	*STE11*	
MAPKK	*STE7*	
MAPK	*FUS3*, *KSS1*	
Transcription factor	*STE12*	Not in the YKO library
Scaffold for shmoo orientation	*FAR1*	
Cdc42 GTPase	*CDC42*	Essential gene
Cdc42-GEF	*CDC24*	Essential gene
Cdc42, Ste5 & Ste20-scaffold	*BEM1*	
Ras GTPase	*RAS1*	
Formins	*BNI1*, *BNR1*	
FUSION COMPONENTS		
Transmembrane Proteins	*PRM1*, *FIG1*, *KEX2*	
Cell wall remodelling	*FUS1*, *FUS2*	
Lipid raft protein	*RVS161*	
Type V myosin	*MYO2*	Not in the YKO library
Tropomyosin	*TPM1*	

312 [a] genes required for the creeping phenotype are shown in red

313 [b] genes whose deletion does not affect the creeping phenotype are shown in black [c]
314 α specific genes are not expected to affect the creeping phenotype in the *MAT***a** gene
315 deletion YKO library context

316 [d] genes that were not present (either missing or essential) in the deletion library are shown
317 in grey

318 * genes whose deletion unexpectedly does not affect the creeping phenotype; see text for
319 discussion

320

321

322 **Functional enrichment and network analyses implicate RIM101 signalling in the creeping**
323 **phenotype**

324 To shed more light on the genetic basis for the creeping phenotype, we performed two further
325 enrichment analyses on our set of 107 genes. First, we used spatial analysis of functional
326 enrichment (SAFE) to investigate how genetic interactions involving the 107 genes relate to
327 the 19 interaction domains previously identified in the yeast genetic interaction landscape
328 (Baryshnikova, 2016, Costanzo *et al.*, 2016). This revealed a concentration of genetic
329 interactions in six functional domains: multivesicular body (MVB) sorting/RIM signalling,
330 mitochondria, chromatin, transcription, metabolism, and cytokinesis (**Figure 5A**).

331 Second, we used NetworkAnalyst (Zhou *et al.*, 2019) to map the 107 genes in a first-order
332 network within an established global network comprised of interactions from the STRING
333 interactome (Szklarczyk *et al.*, 2015). This classified the 107 genes into an interactive network
334 connecting 65 of the 107 genes with eight statistically significant modules ($P < 0.05$)
335 representative of subnetworks that are more interactive than expected at random (**Figure 5B**).
336 To evaluate over-representation of pathways in these modules, an enrichment analysis of
337 interactions for association to the KEGG pathway database was conducted. Five pathways were
338 significantly enriched for five of the modules (**Figure 5B**): MAPK signalling ($P = 1.9 \times 10^{-20}$),
339 ribosome ($P = 5.4 \times 10^{-7}$), endocytosis ($P = 5.0 \times 10^{-4}$), longevity regulating ($P = 7.3 \times 10^{-3}$),
340 and oxidative phosphorylation ($P = 1.6 \times 10^{-5}$). These analyses also show enrichment of mating
341 pathways. For example, the MAPK signalling module (**Figure 5B**) contains many hallmark
342 mating genes (*e.g.*, *STE4*, *STE5*, *STE7*, *STE11*, *STE20*, *STE50*, *GPA1*, *BNI1*, *BNR1*, *BEM1*,
343 and *RAS1*), and is integral to the mating pathway (Bardwell, 2005; **Table 1**). Thus, these
344 modules can provide functional insight into the creeping phenotype.

345 The strongest and most surprising enrichment in both enrichment analyses was for RIM101
346 signalling (auto-annotated in NetworkAnalyst as "endocytosis", presumably because the
347 RIM101 pathway contains ESCRT proteins; **Figure 5**). This enrichment is striking: of the
348 twelve genes in the RIM101 pathway, nine are amongst our 107 gene set (**Figure 6**). Eight of
349 these appear in the NetworkAnalyst analysis (**Figure 5B**). The exception is *YGR122W,* which
350 is required for the creeping phenotype but fell below the NetworkAnalyst protein-protein
351 interaction confidence threshold. *IME1* does not show as required for the creeping phenotype,
352 but, although appearing in NetworkAnalyst endocytosis module, is not considered part of the
353 core RIM101 pathway (Lorenz & Cohen, 2014; **Figure 6**). The remaining two genes, *SNF7*
354 and *SPT22*, were not present in the gene deletion library. Thus, all the core RIM101 pathway
355 genes we could assess are required for the creeping phenotype.

356

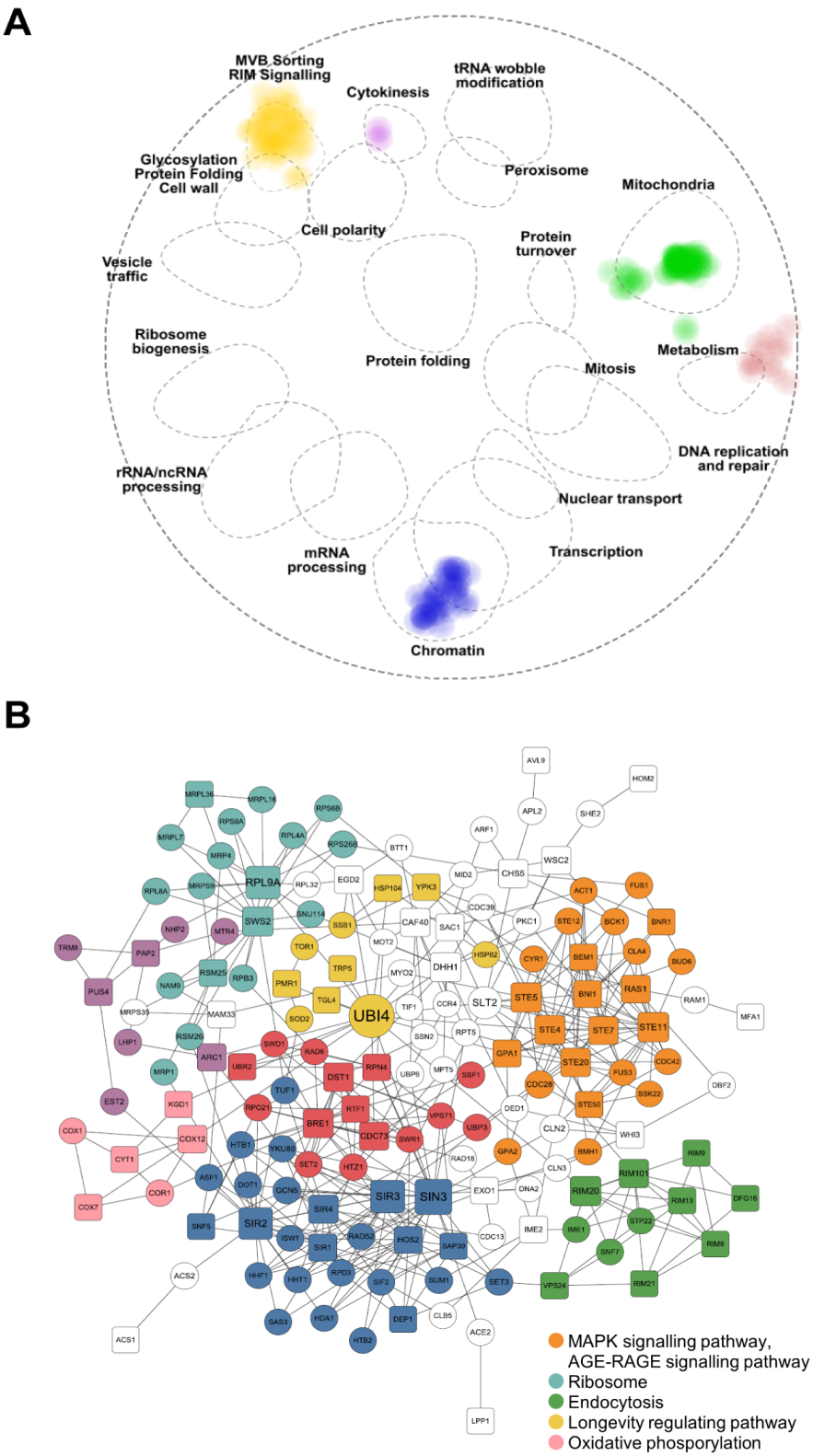

Figure 5: Enrichment analyses of genes required for the creeping phenotype. (A) Spatial analysis of functional enrichment (SAFE) of the 107 deletion strains required for the creeping phenotype. All 107 genes were mapped in an established genetic interaction network to identify over-represented regions. The 107 genes show

361 significant membership to six of the previously defined 19 functional regions (Baryshnikova, 2016, Costanzo *et*
362 *al.*, 2016), illustrated by dotted ellipses, with the intensity of color proportional to the number of genes. (**B**)
363 Pathway enrichment for first-order minimum network analysis of the genes required for the creeping phenotype.
364 65 of the 107 genes appear in this network. Genes required for creeping phenotype are shown as square nodes;
365 interacting genes as circular nodes. The first-order network was generated in NetworkAnalyst (Zhou *et al.*, 2019)
366 with the STRING interactome database where nodes and edges represent genes and genetic/physical interactions,
367 respectively. Node size is based on betweenness score, which is indicative of node importance for overall network
368 connectivity. Nodes are colored by module analysis representing tightly clustered subnetworks with more internal
369 connections than randomly expected in the whole network. Nodes not assigned to a module are without color. The
370 most significantly enriched pathway (lowest *P*-value less than 0.05) in the KEGG database was identified for each
371 module. Modules indicated in the legend at bottom right had significant pathway enrichment ($P < 0.05$), while
372 those not listed in the legend did not.

373

374 The RIM101 pathway is a conserved fungal-specific signalling pathway that mediates
375 adaptation to external pH (Penalva & Arst, 2004). It is named after the pH-responsive
376 transcription factor Rim101 whose activation by C-terminal proteolytic cleavage is the key
377 output of the pathway (Orejas *et al.*, 1995, Li & Mitchell, 1997; **Figure 6**). Besides its role in
378 environmental pH response, the pathway is involved in diverse cellular behaviors that include
379 sporulation and haploid invasive growth in *S. cerevisiae* (Su & Mitchell, 1993, Li & Mitchell,
380 1997), salt tolerance in *S. cerevisiae* and *Candida albicans* (Lamb & Mitchell, 2003),
381 pathogenicity in *C. albicans*, *Aspergillus fumigatus* and *Cryptococcus neoformans* (Davis,
382 2009), and cell wall assembly in *S. cerevisiae* and *C. neoformans* (Castrejon *et al.*, 2006,
383 O'Meara *et al.*, 2013, Zhao *et al.*, 2019).

384 Involvement of the RIM101 pathway in the creeping phenotype of *S. cerevisiae* mating cells
385 strongly suggests that this signalling pathway also plays an important role in the first step(s) of
386 mating, particularly in mating partner aggregation (**Figure 4**, **Supplementary Figure 4**). We

387 hypothesize that the RIM101 pathway mediates this process by regulating expression of **a**
388 and α agglutinin encoding genes, given Rim101 is a transcription factor. While we are not
389 aware of the RIM101 pathway having previously been proposed to mediate mating in *S.*
390 *cerevisiae, rim* mutants have been reported to display mating defects (Castrejon *et al.*, 2006).
391 Direct support for our hypothesis comes from results showing that deletion of *RIM101* and
392 *RIM13* (encoding the protease responsible for Rim101 activation; **Figure 6**) both result in
393 downregulated expression of *AGA2* and *MFA1* (which encode the **a**-agglutinin adhesive
394 subunit and pheromone **a**, respectively) in a *MAT***a** strain (Lamb & Mitchell, 2003;
395 **Supplementary Table 5**). In addition, when we examined a publicly-available genome-wide
396 RNA-seq dataset where *RIM101* is deleted in a *MAT*α strain (Read *et al.*, 2016), we found that
397 the α-agglutinin and pheromone α encoding genes (*SAG1*, *MF(ALPHA)1*, *MF(ALPHA)2*) were
398 significantly downregulated, mirroring the impact of *RIM101* deletion in a *MAT***a** strain
399 (**Supplementary Table 5**). These data also show downregulation of *AGA1,* encoding the **a**-
400 agglutinin anchor subunit in the *MAT*α context (**Supplementary Table 5**), which is likely an
401 outcome of *AGA1* being expressed in both *MAT***a** and *MAT*α cells (Lipke & Kurjan, 1992).
402 Thus, Rim101 seems to regulate expression of mating aggregation genes in both mating types.
403 Moreover, expression of *RIM101* is absolutely required in both partners for mating in the yeast
404 *Yarrowia lipolytica* (Lambert *et al.*, 1997), although the mating was assessed on solid rather
405 than liquid medium. Finally, **Supplementary Table 5** shows that around 2/3rds (19 out of 30)
406 of the genes reported to be involved in mating signalling (Merlini *et al.*, 2013) have their
407 expression significantly affected by *RIM101* deletion, suggesting a wider involvement of the
408 RIM101 pathway in mating. Altogether, our data and existing evidence suggest a novel and
409 direct role for the *RIM101* signalling pathway in sexual agglutinin expression as part of a more
410 general role in mating signalling, thereby explaining the involvement of this pathway in the
411 creeping phenotype.

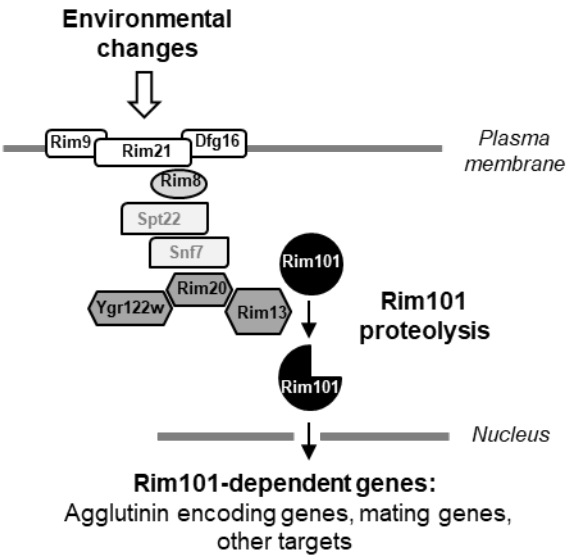

Figure 6: Schematic representation of the RIM101 signalling pathway and its potential involvement in *S. cerevisiae* mating. The fungal-specific RIM101 signalling pathway is based on the proteolytic processing of the Rim101 transcription factor. The integral membrane proteins Rim21, Dfg6 and Rim9 constitute a surface response complex that recruits the arrestin-like Rim8 at the plasma membrane. Downstream ESCRT (Endosomal Sorting Complex Required for Transport) proteins Spt22, Vsp24, Snf7 are recruited in a Rim8-dependent manner to constitute a platform on which the proteolytic complex (Ygr122w, Rim20, Rim13) forms. The calpain-like cysteine protease Rim13 then cleaves Rim101, inducing its nuclear localization and cellular transcriptional response. We propose that Rim101 targets include genes responsible for the sexual agglutination response amongst other genes that mediate mating. Apart from *SNF7* and *SPT22*, which were not present in our gene deletion library screen, all genes in the RIM101 pathway were found to be required for the creeping phenotype (**Figure 5B**, **Supplementary Table 3**). Adapted from Ost *et al.* (2015).

426 **Conclusions**

427 Here we describe a rapid, inexpensive and robust method to determine not only the mating type
428 of an unknown *S. cerevisiae* strain, but also whether the strain is haploid or diploid. While we
429 serendipitously discovered the creeping phenotype in our laboratory, we have heard
430 anecdotally that we are not the first to discover it and that it is currently used as a mating type
431 assay in some laboratories. Thus, here we focused on evaluating and optimizing the phenotype
432 to provide it as an alternative mating type assay for the yeast community. The assay is as simple
433 as mixing an "unknown" sample with known *MAT***a** and *MAT*α strains at roughly equal cell
434 densities and observing the results after 18 hours, thus it is cheap, robust, and requires minimal
435 hands-on time. So far, all *S. cerevisiae* strains we have tried in our laboratory are amenable to
436 the assay, but we do not know whether it will work for all *S. cerevisiae* strains or for other
437 *Saccharomyces* species.

438 Our microscopy data suggest the phenotype results from cell aggregation that occurs during
439 yeast mating. This conclusion is supported by the timing of the creeping phenotype, which
440 occurs around the start of mating following mixing of compatible strains and is concomitant
441 with visible signs of aggregation. It is also consistent with the requirement for conditions
442 facilitating growth, and in particular with the longevity of the phenotype - well past when
443 mating is likely to have completed. Moreover, demonstration that the creeping phenotype
444 depends on many characterized mating genes, and in particular on the *AGA1* and *AGA2*
445 agglutinin genes, is also consistent with aggregation underlying the phenotype.

446 Surprisingly, our functional genomics screen identified the RIM101 pathway as being
447 necessary for the creeping phenotype. All components of this pathway we could assess (all
448 three surface response complex genes *RIM9*, *RIM21*, and *DFG16*; two of the four of Rim8-
449 dependent platform component genes (*RIM8, VSP24*); and all thee proteolytic complex genes

450 *RIM13*, *RIM20*, *YGR122w*) are required for the creeping phenotype. The gene encoding the
451 transcription factor Rim101 is also required, proteolytic activation of which is the key output
452 of the pathway. We suggest that Rim101 regulates the agglutinin genes, thus dependence of
453 the creeping phenotype on the RIM101 pathway can be explained simply by a decrease of the
454 expression of these genes in the absence of Rim101 activation. Our examination of published
455 data supports this contention, and a more general, previously-unrecognized role for RIM101
456 signalling in *S. cerevisiae* mating. While Rim101-dependent regulation of the agglutinin genes
457 can explain the dependence of the creeping phenotype on the RIM101 pathway, the trigger that
458 leads to Rim101 activation during mating is unknown. Thus, future work will be required to
459 confirm whether Rim101 directly regulates the agglutinin genes and other mating genes, and
460 how the RIM101 pathway is activated during mating. The simplicity of assaying the creeping
461 phenotype will aid these future approaches, as well as further investigations into the phenotype.

462

463 **Funding**
464 This work was supported by a grant from the New Zealand Marsden Fund [10-MAU-072] to
465 ARDG.

466

467 **Acknowledgements**

468 We thank Ganley lab members for comments on the manuscript.

469 **References**

470 Banderas A, Koltai M, Anders A & Sourjik V (2016) Sensory input attenuation allows predictive
471 sexual response in yeast. *Nature Communications* **7**: 12590.
472 Bardwell L (2005) A walk-through of the yeast mating pheromone response pathway. *Peptides* **26**:
473 339-350.
474 Baryshnikova A (2016) Systematic functional annotation and visualization of biological networks.
475 *Cell Systems* **2**: 412-421.
476 Botstein D & Fink GR (2011) Yeast: an experimental organism for 21st Century biology. *Genetics*
477 **189**: 695-704.
478 Bradbury JE, Richards KD, Niederer HA, Lee SA, Rod Dunbar P & Gardner RC (2006) A
479 homozygous diploid subset of commercial wine yeast strains. *Antonie Van Leeuwenhoek* **89**: 27-37.
480 Burkholder AC & Hartwell LH (1985) The yeast alpha-factor receptor: structural properties deduced
481 from the sequence of the *STE2* gene. *Nucleic Acids Res* **13**: 8463-8475.
482 Busby BP, Niktab E, Roberts CA, Sheridan JP, Coorey NV, Senanayake DS, Connor LM, Munkacsi
483 AB & Atkinson PH (2019) Genetic interaction networks mediate individual statin drug response in
484 *Saccharomyces cerevisiae*. *npj Systems Biol Applic* **5**: 35.
485 Castrejon F, Gomez A, Sanz M, Duran A & Roncero C (2006) The RIM101 pathway contributes to
486 yeast cell wall assembly and its function becomes essential in the absence of mitogen-activated
487 protein kinase Slt2p. *Eukaryot Cell* **5**: 507-517.
488 Chen EY, Tan CM, Kou Y, Duan Q, Wang Z, Meirelles GV, Clark NR & Ma'ayan A (2013) Enrichr:
489 interactive and collaborative HTML5 gene list enrichment analysis tool. *BMC Bioinformatics* **14**: 128.
490 Chen P, Sapperstein SK, Choi JD & Michaelis S (1997) Biogenesis of the *Saccharomyces cerevisiae*
491 mating pheromone a-factor. *J Cell Biol* **136**: 251-269.
492 Costanzo M, VanderSluis B, Koch EN*, et al.* (2016) A global genetic interaction network maps a
493 wiring diagram of cellular function. *Science* **353**: aaf1420.
494 Cubillos FA, Louis EJ & Liti G (2009) Generation of a large set of genetically tractable haploid and
495 diploid *Saccharomyces* strains. *FEMS Yeast Res* **9**: 1217-1225.

496 Davis DA (2009) How human pathogenic fungi sense and adapt to pH: the link to virulence. *Curr*
497 *Opin Microbiol* **12**: 365-370.
498 Duntze W, MacKay V & Manney TR (1970) *Saccharomyces cerevisiae*: a diffusible sex factor.
499 *Science* **168**: 1472-1473.
500 Giaever G & Nislow C (2014) The yeast deletion collection: a decade of functional genomics.
501 *Genetics* **197**: 451-465.
502 Guthrie C & Fink GR (1991) Guide to Yeast Genetics and Molecular Biology. Vol. 194 Academic
503 Press, San Diego.
504 Haber JE (2012) Mating-type genes and *MAT* switching in *Saccharomyces cerevisiae*. *Genetics* **191**:
505 33-64.
506 Herskowitz I & Jensen RE (1991) Putting the *HO* gene to work: Practical uses for mating-type
507 switching. *Methods Enzymol* **194**: 132-146.
508 Jahng KY, Ferguson J & Reed SI (1988) Mutations in a gene encoding the alpha subunit of a
509 *Saccharomyces cerevisiae* G protein indicate a role in mating pheromone signaling. *Mol Cell Biol* **8**:
510 2484-2493.
511 Kanehisa M & Goto S (2000) KEGG: kyoto encyclopedia of genes and genomes. *Nucleic Acids Res*
512 **28**: 27-30.
513 Kanehisa M, Furumichi M, Sato Y, Ishiguro-Watanabe M & Tanabe M (2021) KEGG: integrating
514 viruses and cellular organisms. *Nucleic Acids Res* **49**: 545-551.
515 Kuleshov MV, Jones MR, Rouillard AD*, et al.* (2016) Enrichr: a comprehensive gene set enrichment
516 analysis web server 2016 update. *Nucleic Acids Res* **44**: 90-97.
517 Lamb TM & Mitchell AP (2003) The transcription factor Rim101p governs ion tolerance and cell
518 differentiation by direct repression of the regulatory genes *NRG1* and *SMP1* in *Saccharomyces*
519 *cerevisiae*. *Mol Cell Biol* **23**: 677-686.
520 Lambert M, Blanchin-Roland S, Le Louedec F, Lepingle A & Gaillardin C (1997) Genetic analysis of
521 regulatory mutants affecting synthesis of extracellular proteinases in the yeast *Yarrowia lipolytica*:
522 identification of a *RIM101/pacC* homolog. *Mol Cell Biol* **17**: 3966-3976.

523 Li W & Mitchell AP (1997) Proteolytic activation of Rim1p, a positive regulator of yeast sporulation
524 and invasive growth. *Genetics* **145**: 63-73.
525 Lipke PN & Kurjan J (1992) Sexual agglutination in budding yeasts: structure, function, and
526 regulation of adhesion glycoproteins. *Microbiol Rev* **56**: 180-194.
527 Liti G, Carter DM, Moses AM*, et al.* (2009) Population genomics of domestic and wild yeasts. *Nature*
528 **458**: 337-341.
529 Lorenz K & Cohen BA (2014) Causal variation in yeast sporulation tends to reside in a pathway
530 bottleneck. *PLoS Genet* **10**: e1004634.
531 Merlini L, Dudin O & Martin SG (2013) Mate and fuse: how yeast cells do it. *Open Biology* **3**:
532 130008.
533 Michaelis S & Herskowitz I (1988) The a-factor pheromone of *Saccharomyces cerevisiae* is essential
534 for mating. *Mol Cell Biol* **8**: 1309-1318.
535 O'Meara TR, Holmer SM, Selvig K, Dietrich F & Alspaugh JA (2013) *Cryptococcus neoformans*
536 Rim101 is associated with cell wall remodeling and evasion of the host immune responses. *mBio* **4**:
537 e00522-00512.
538 Orejas M, Espeso EA, Tilburn J, Sarkar S, Arst HN & Penalva MA (1995) Activation of the
539 *Aspergillus* PacC transcription factor in response to alkaline ambient pH requires proteolysis of the
540 carboxy-terminal moiety. *Genes Dev* **9**: 1622-1632.
541 Ost KS, O'Meara TR, Huda N, Esher SK & Alspaugh JA (2015) The *Cryptococcus neoformans*
542 alkaline response pathway: identification of a novel rim pathway activator. *PLoS Genet* **11**: e1005159.
543 Penalva MA & Arst HN (2004) Recent advances in the characterization of ambient pH regulation of
544 gene expression in filamentous fungi and yeasts. *Annu Rev Microbiol* **58**: 425-451.
545 Read T, Richmond PA & Dowell RD (2016) A trans-acting variant within the transcription factor
546 RIM101 interacts with genetic background to determine its regulatory capacity. *PLoS Genet* **12**:
547 e1005746.
548 Sena EP, Radin DN & Fogel S (1973) Synchronous mating in yeast. *PNAS* **70**: 1373-1377.
549 Sherman F (1991) Getting started with yeast. *Methods Enzymol* **194**: 3-21.
550 Sprague GFJ (1991) Assay of yeast mating reaction. *Methods Enzymol* **194**: 77-93.

551 Su SS & Mitchell AP (1993) Identification of functionally related genes that stimulate early meiotic
552 gene expression in yeast. *Genetics* **133**: 67-77.
553 Szklarczyk D, Franceschini A, Wyder S*, et al.* (2015) STRING v10: protein-protein interaction
554 networks, integrated over the tree of life. *Nucleic Acids Res* **43**: 447-452.
555 Treco DA & Lundblad V (1993) Preparation of yeast media. *Curr Protoc Mol Biol* **23**: 13.11.11-
556 13.11.17.
557 Zhao F, Li J, Lin K, Chen H, Lin Y, Zheng S, Liang S & Han S (2019) Genome-wide screening of
558 *Saccharomyces cerevisiae* deletion mutants reveals cellular processes required for tolerance to the cell
559 wall antagonist calcofluor white. *Biochem Biophys Res Commun* **518**: 1-6.
560 Zhao H, Shen ZM, Kahn PC & Lipke PN (2001) Interaction of alpha-agglutinin and a-agglutinin,
561 *Saccharomyces cerevisiae* sexual cell adhesion molecules. *J Bacteriol* **183**: 2874-2880.
562 Zhou G, Soufan O, Ewald J, Hancock REW, Basu N & Xia J (2019) NetworkAnalyst 3.0: a visual
563 analytics platform for comprehensive gene expression profiling and meta-analysis. *Nucleic Acids Res*
564 **47**: 234-241.

565